



Published in final edited form as:

Circ Cardiovasc Interv. 2022 December ; 15(12): e011928. doi:10.1161/
CIRCINTERVENTIONS.122.011928.

Native and Post-Repair Residual Mitral Valve Prolapse Increases Forces Exerted on the Papillary Muscles: A Possible Mechanism for Localized Fibrosis?

Matthew H. Park, MS^{1,2,*}, Antonia van Kampen, MD^{3,4,5,*}, Serguei Melnitchouk, MD, MPH³, Robert J. Wilkerson, BS¹, Yasufumi Nagata, MD, PhD⁴, Yuanjia Zhu, MD, MS^{1,6}, Hanjay Wang, MD¹, Pearly K. Pandya, MS^{1,2}, Jordan E. Morningstar, BS⁷, Michael A. Borger, MD, PhD⁵, Robert A. Levine, MD⁴, Y. Joseph Woo, MD^{1,6}

¹Department of Cardiothoracic Surgery, Stanford University, Stanford, CA

²Department of Mechanical Engineering, Stanford University, Stanford, CA

³Division of Cardiac Surgery, Massachusetts General Hospital, Harvard Medical School, Boston, Massachusetts

⁴Cardiac Ultrasound Laboratory, Massachusetts General Hospital, Harvard Medical School, Boston, Massachusetts

⁵University Department of Cardiac Surgery, Leipzig Heart Center, Leipzig, Germany

⁶Department of Bioengineering, Stanford University, Stanford, CA

⁷Department of Regenerative Medicine and Cell Biology, Medical University of South Carolina, Charleston, SC

Abstract

Background: Recent studies have linked mitral valve prolapse to localized myocardial fibrosis, ventricular arrhythmia, and even sudden cardiac death independent of mitral regurgitation or hemodynamic dysfunction. The primary mechanistic theory is rooted in increased papillary muscle traction and forces due to prolapse, yet no biomechanical evidence exists showing increased forces. Our objective was to evaluate the biomechanical relationship between prolapse and papillary muscle forces, leveraging advances in *ex vivo* modeling and technologies.

We hypothesized that mitral valve prolapse with limited hemodynamic dysfunction leads to significantly higher papillary muscle forces, which could be a possible trigger for cellular and electrophysiological changes in the papillary muscles and adjacent myocardium.

Corresponding Author: Y. Joseph Woo, M.D., Norman E. Shumway Professor and Chair, Department of Cardiothoracic Surgery, Professor, by courtesy, Department of Bioengineering, Stanford University, Falk Cardiovascular Research Building CV-235, 300 Pasteur Drive, Stanford, CA 94305-5407, Phone: 650-725-3828, Fax: 650-736-0901, joswoo@stanford.edu.

*Co-first authors: Authors contributed equally

Disclosures

The authors have nothing to disclose and report no conflicts of interest

Supplemental Material

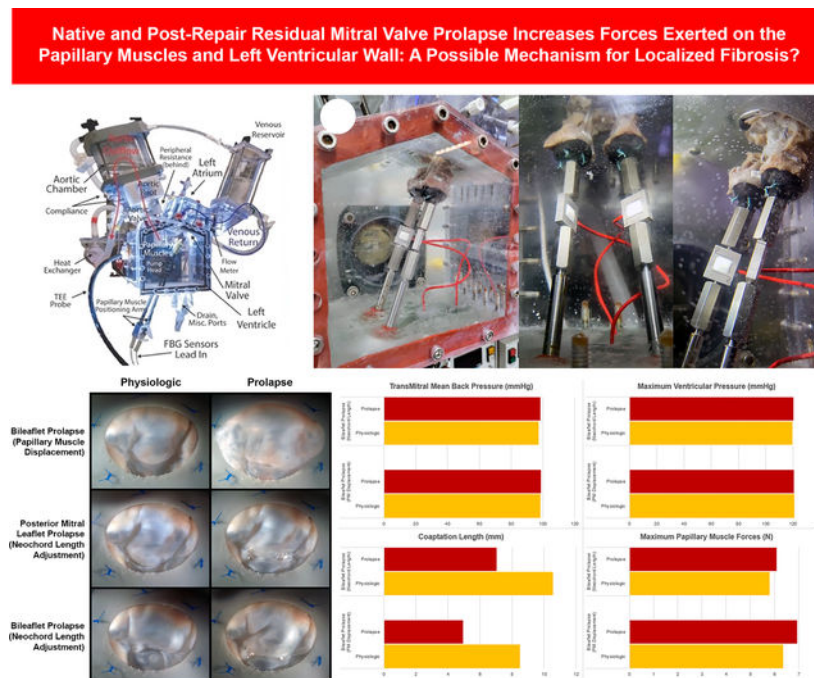
Table S1–S3

Methods: We developed an *ex vivo* papillary muscle force transduction and novel neochord length adjustment system capable of modeling targeted prolapse. Using 3 unique ovine models of mitral valve prolapse (bileaflet or posterior leaflet prolapse), we directly measured hemodynamics and forces, comparing physiologic and prolapsing valves.

Results: We found that bileaflet prolapse significantly increases papillary muscle forces by 5% to 15% compared with an optimally coapting valve, which are correlated with statistically significant decreases in coaptation length. Moreover, we observed significant changes in the force profiles for prolapsing valves when compared with normal controls.

Conclusions: We discovered that bileaflet prolapse with the absence of hemodynamic dysfunction results in significantly elevated forces and altered dynamics on the papillary muscles. Our work suggests that the sole reduction of mitral regurgitation without addressing reduced coaptation lengths and thus increased leaflet surface area exposed to ventricular pressure gradients (i.e., billowing leaflets) is insufficient for an optimal repair.

Graphical Abstract



Keywords

ex vivo heart modeling; mitral valve prolapse; papillary muscle forces; neochordal repair; cardiac biomechanics

Keywords

Arrhythmias; Animal Models of Human Disease; Fibrosis; Hemodynamics; Pathophysiology; Cardiovascular Surgery; Valvular Heart Disease

Introduction

Mitral valve prolapse (MVP) is a very common pathology that describes the superior displacement or bulging of the mitral valve (MV) leaflets into the left atrium during systole,¹ and it is the most common cause of isolated mitral regurgitation (MR) requiring surgical repair.²⁻⁴ MVP usually presents as isolated posterior mitral leaflet (PML) prolapse or bileaflet prolapse and is associated with frequent and serious complications, including stroke and heart failure.^{1,4,5} However, recent studies have linked the condition to sudden cardiac death in younger individuals, occurring as a result of ventricular arrhythmia, even in the absence of severe MR.^{6,7} This arrhythmia is related to localized fibrosis and scarring of the left ventricular myocardium and papillary muscles (PMs), and histological autopsy studies found scarring at the level of the PMs, adjacent free wall, and inferobasal wall in all young sudden cardiac death victims with MVP,^{6,8} whereas biopsies of MVP patients found regionalized fibrosis, markedly increased compared with septal and apical biopsies.⁹ Taken in combination with imaging data that show superior PM displacement and abnormal systolic motions of the inferobasal myocardium in MVP patients,^{10,11} the existing evidence strongly suggests that prolapse, independent of MR, alters the biomechanical performance of the valve and surrounding myocardium.

The primary theory explaining the observation of localized fibrosis in patients with MVP in the absence of MR is rooted in increased PM traction force from prolapse. This force is transferred to the PMs via the chordae tendineae causing myocardial stretch, which activates mechanically-induced biological signaling cascades leading to fibrosis.^{6,12,13} Recent studies have even brought attention to progressive superior shift of the MV during systole observed via echocardiography, suggesting an augmented superiorly oriented force due to the systolic left ventricular pressure.¹³ Despite these observations, no biomechanical evidence exists explicitly showing increased forces on the PMs due to MVP, and to better understand this increasingly relevant disease, we aimed to evaluate the biomechanical relationship between prolapse and PM force using *ex vivo* technologies.¹⁴

We developed a comprehensive PM force transduction system for use during heart modeling and a novel neochord length adjustment system capable of recreating targeted prolapse. We hypothesized that MVP with limited hemodynamic dysfunction leads to significantly higher PM forces, providing a biomechanically-based mechanism for the localized stretch-induced changes in myocardial biology observed in a significant portion of MVP patients. Our *ex vivo* results establish the basis of advanced understanding of MVP biomechanics, creating a platform for further work aimed at interventional treatment opportunities and advanced clinical guidelines for this lethal disease.

Methods

The authors declare that all supporting data are available within the article.

Ex Vivo Left Heart Modeling

MVs (n=10) were explanted from healthy ovine hearts obtained from an abattoir and mounted in a left heart simulator as previously described and validated (Figure 1A).^{15,16}

The use of ovine cardiac tissue from an abattoir is exempt from committee approval, and all experiments were performed in accordance with institutional guidelines. Our left heart flow loop features a linear piston pump (Superpump, ViVibro Labs, Victoria, BC, Canada) used to generate physiologic hemodynamics, with effective stroke volumes of 70 mL at 70 bpm programmed in accordance with ISO 5840 standards for *ex vivo* valve testing. Mitral flow was recorded with an electromagnetic flow probe, and ventricular, aortic, and atrial pressures were measured using pressure transducers. For each sample compliance chambers and adjustable peripheral resistance were titrated to produce mean arterial pressures of 100 mmHg, and hemodynamic data were collected and averaged across 10 cardiac cycles.

Papillary Muscle Force Transducers

PMs were excised from the left ventricle, leaving ~2 to 3 cm of the distal ends, and were fixed to 3D-printed mounts with 4 pledgeted GoreTex (W.L. Gore, Newark, DE) sutures. The mounts were integrated with submersible force transducers (LSB210, FUTEK, Irvine, CA), all of which were fixed to stainless steel rods transecting the bottom of the ventricular chamber (Figure 1B). The force sensors were calibrated with precision weights in both tension and compression. In combination with strain gauge amplifiers (IDA100, FUTEK), recording at a sampling rate of 1.2 kHz with 15 noise-free bits, the ultimate resolution of our system was on the order of hundreds of μN .

Neochord Length Adjustment System

We created a novel length adjustment system for implanted neochordae spanning the leaflets and PMs, allowing us to precisely lengthen or shorten neochordae without re-performing surgical implantation, improving experimental control and maintaining insertion points between conditions. The system consisted of a custom PM mount integrated with a series of 3D-printed interlocking pledgets. With a layer height resolution of 25 μm , each pledget was printed with a thickness of 1.5 mm in an epoxy-based resin. The pledgets contained 4 embossed and debossed cylinder features for vertical stacking and lateral channels for fixing neochordae within the adjustment system (Figure 2A). Upon implantation, GoreTex sutures were threaded through the pledgets, PM mounts, PMs, and leaflets, allowing us to adjust neochord lengths in multiples of 1.5 mm, which we used to precisely tune our leaflet-specific prolapse models (Figure 2B).

Data Analysis

For each sample, we recorded hemodynamic, echocardiographic, and PM force data. PM forces were evaluated as aggregate metrics of both PMs, removing distribution as a confounding variable. Hemodynamic metrics were evaluated using the ViVitest application and custom Python scripts utilizing the numpy, pandas, scipy, and matplotlib libraries. We collected echocardiographic data using a Phillips iE33 system and S5-1 transthoracic probe (Koninklijke Philips NV, Amsterdam, The Netherlands), and from parasternal long axis images, measured the coaptation length of each valve.

Experimental Procedures

To comprehensively model MVP biomechanics, we designed our experiments in a staged, paired manner, using 3 different models. For each sample, we collected hemodynamic, PM force, high-speed videographic, and echocardiographic data as described above. We randomized the order of conditions for each experimental set to avoid confounding time-dependent changes in tissue properties. For each state, we titrated systemic resistances to maintain identical pressures between conditions as pressures alter PM forces.^{17,18} Regurgitation was minimized to mild or moderate levels in the prolapse state (<25%).

For the first set of experiments (E-I), we evaluated MV biomechanics using a bileaflet prolapse model generated via vertical displacement of the PMs (n=10). Valve mechanics were evaluated in a physiologic state, with PMs positioned at a physiologic distance to the mounted annulus that resulted in little to no prolapse or tethering, and a raised state, with PMs positioned at a reduced distance to the annulus (Figure 3A). The raised state replicates prolapse via chordal elongation because reduced leaflet to PM distances superiorly translate the chordae and simulate relatively longer lengths, resulting in pathological prolapse similar to our previously validated Barlow disease model.¹⁹

For the second set of experiments (E-II), we evaluated MV biomechanics for an isolated PML prolapse model using our novel neochord length adjustment system. Using the same valves from E-I with PM positions at the physiologic state, P2 primary chordae were excised from the PML and replaced with two CV-5 neochordae, one to each PM (n=8). By adding or removing pledgets, we tuned neochord lengths to a physiologic or prolapse state (Figure 3B). The physiologic state was determined as the point of optimal coaptation, evaluated via high-speed videography and echocardiography, whereas the prolapse state was determined as the point of minimal echocardiographic coaptation length while maintaining at most, mild to moderate regurgitation (<25%).

For the final set of experiments (E-III), we evaluated MV biomechanics for another bileaflet prolapse model using our neochord length adjustment system. Using the same valves and fixed PM configurations from E-II, A2 primary chordae from the anterior mitral leaflet were excised and replaced with 2 CV-5 neochordae, one to each PM (n=8) (Figure 3C). These modifications were performed in addition to the modifications performed for the valves from E-II, resulting in MVs with a total of 4 adjustable length neochordae, 1 each spanning the 2 PMs and 2 leaflets. E-I focused on creating a generalized pathological disease model, whereas E-III aimed to simulate a post-neochordal-repair prolapse condition where bileaflet prolapse remains despite reduction in MR. Once again, neochord lengths were evaluated in physiologic and prolapse states, determined using a combination of echocardiographic, videographic, and hemodynamic metrics.

Statistical Methods

Statistical significance was defined at $p < 0.05$ for all tests and continuous variables are reported as mean \pm standard error. Assuming normally distributed data, confirmed with Shapiro-Wilk normality tests ($p > 0.05$ for all metrics), we performed paired, 2-tailed Student t tests to compare continuous variables between groups.

Results

E-I: Bileaflet Prolapse from Papillary Muscle Displacement

Hemodynamic data for the prolapse and physiologic conditions revealed nearly identical maximum ventricular pressures and transmitral pressure gradients (Figure 4A, Table S1). While prolapsing valves showed statistically significant increases in MR compared with that of physiologic valves (19.11 ± 1.53 , 10.61 ± 0.55 , respectively; $p<0.001$), the regurgitation levels remained within a range of mild severity ($<20\%$). Coaptation length was significantly decreased for prolapsing valves compared with that of physiologic valves (4.98 ± 0.48 mm, 8.52 ± 0.40 mm, respectively; $p<0.001$).

Despite similar maximum systolic pressures, we saw a significant increase in peak PM forces of 9.23% for prolapsing valves compared with those of physiologic valves (6.95 ± 0.41 N, 6.37 ± 0.37 N, respectively; $p=0.002$) (Table S1). Aggregate PM force data showed a double peak profile, similar to PM and chordal force data of previous studies (Figure 5A).^{16,18,20,21} Prolapsing valves showed significantly higher primary peak magnitudes of 13.86% compared with those of physiologic valves (6.85 ± 0.42 N, 6.01 ± 0.39 N, respectively; $p<0.001$), corresponding to a significant decrease in the force time derivative ($d\vec{F}/dt$) of the primary peak, as primary peaks occurred in identical time-domains ($p<0.001$). Moreover, when evaluated relative to their own secondary peak magnitudes, prolapsing valves showed an average of 1.59% higher primary peak magnitudes, whereas physiologic valves showed 4.90% lower primary peak magnitudes, indicating a fundamental difference in force profiles.

E- II: Isolated Posterior Mitral Leaflet Prolapse from Neochord Length Adjustment

Hemodynamic data for prolapse and physiologic conditions revealed close similarity with statistical acceptance of the null hypothesis for all highlighted metrics (Figure 4B, Table S2). Although there were significant differences in MR between physiologic and prolapse conditions (11.43 ± 1.25 , 12.80 ± 1.23 , respectively; $p=0.042$), the difference was a negligible 1.37% of regurgitation and both conditions remained within mild severity. Coaptation length was statistically insignificant between physiologic and prolapsing valves (10.15 ± 0.48 mm, 9.47 ± 0.39 mm, respectively; $p=0.094$), and the average difference in neochord length between conditions was ~ 4.5 mm.

While prolapsing valves had significantly higher primary peak forces ($p=0.044$), overall maximum PM force magnitudes were not significantly changed between physiologic and prolapsing valves ($p=0.051$), although prolapsing valves had slightly higher magnitudes, 1.50% greater, than those of physiologic valves (Table S2). Additionally, we did not see any significant differences in primary peak magnitudes or $d\vec{F}/dt$ (Figure 5B).

E-III: Bileaflet Prolapse from Neochord Length Adjustment

For our bileaflet prolapse neochord model, we confirmed that hemodynamic data for prolapse and physiologic conditions were closely mirrored with statistical acceptance of the null hypothesis for all highlighted metrics (Figure 4C, Table S3). There were no significant differences in MR between physiologic and prolapse conditions, with 16.22%

± 2.20 and $15.29\% \pm 1.67$, respectively, and similarly to E-II, the average difference in neochord length between prolapsing and physiologic valves was ~ 4.5 mm. Coaptation length was significantly decreased for prolapsing valves compared with those of physiologic valves (7.05 ± 0.45 mm, 10.59 ± 0.36 mm, respectively; $p < 0.001$).

In E-III, PM force magnitudes were significantly higher for prolapsing valves when compared with those of physiologic valves (6.10 ± 0.39 N, 5.82 ± 0.43 N, respectively), correlating to a 5.49% increase for prolapsing valves ($p = 0.013$) (Table S3). Moreover, while the bileaflet prolapse condition resulted in significantly higher primary and secondary peak forces ($p = 0.003$, $p = 0.004$, respectively) force profiles did not vary significantly with no significant differences in primary to secondary peak distributions between conditions (Figure 5C).

Discussion

To the best of our knowledge, no directly measured biomechanical evidence exists suggesting increased forces on the PMs due to isolated prolapse in the absence of severe MR; yet this connection has been implicated in numerous imaging and histological studies.^{6,8–11,13,22} To evaluate this theory, we developed comprehensive PM force transduction and neochord length adjustment systems capable of creating targeted prolapse. For both isolated PML and bileaflet prolapse, our results are the first to show elevated PM forces as a direct result of MVP in absence of hemodynamic dysfunction, establishing the basis for more advanced understanding of the biomechanical changes involved in MVP and creating a platform for further work aimed at developing interventional treatments and advancing clinical guidelines for this lethal disease.

In analyzing our results, we found that bileaflet prolapse in both our PM displacement and neochord length adjustment models leads to significantly increased PM forces of 5% to 15%. Although these relatively marginal changes could be clinically irrelevant, it has been shown that long-term mechanical fatigue damage scales exponentially with cyclic peak stresses due to cumulative properties of fatigue.²³ Specifically for chordae, based on a previously published power law curve, a 5% increase in forces could reduce the number of cycles to failure by 19.11%.²³

In addition to significant changes in maximum force magnitudes, we observed fundamental differences in the force profiles for prolapsing valves in our PM displacement model, with a higher distribution of force at primary peaks, leading to increased primary peak $d\vec{F}/dt$. These differences are similar to what has been reported for papillary versus apical mounting of neochordae, which has been linked to increased failure of transapically mounted neochordae.¹⁵ The relatively increased primary peak $d\vec{F}/dt$ magnitudes have been suggested to create a whipping phenomenon, similar to towline instability, and a more dynamic loading profile, both of which play significant roles in the stress mechanics due to the rate dependence of the stress-strain relationship for viscoelastic materials.¹⁵

Additionally, while MR levels between models were not always statistically insignificant, our results indicate a high likelihood of statistical decoupling from the force results. The primary reason for increased MR levels in E-II and E-III is that these experimental conditions attempt to recreate a physiologic valve after induction of an acute chordal rupture model, and each experiment introduces further MR from progressive native chordal excision and neochordal implantation. Although we would assume that increased regurgitation plays a role on force dynamics, transvalvular and ventricular pressures ultimately drive these initial force magnitudes which remained constant between samples and experiments. Moreover, the MR levels seen with prolapsing valves would never be clinically interpreted as severely pathological requiring intervention, making our results that relative PM forces are significantly higher especially surprising.

Although we saw significant force increases in our bileaflet prolapse models, we did not observe these same differences for our isolated PML prolapse model. However, when analyzing the videographic and echocardiographic data, we observed that lengthening of PML neochordae did not consistently induce the reduction in coaptation length and billowing leaflet phenotype of prolapse that we clearly observed in our bileaflet models. Instead, lengthening of only PML neochordae often shifted the coaptation surface anteriorly (Figure 6). These observations are corroborated in the representative echocardiographic images, with prolapsing valves from E-I and E-III showing superior leaflet protrusion relative to the annulus and prolapsing valves in E-II not showing such a clear difference (Figure 7). Although it may be true that isolated PML prolapse does not have as large of a clinical effect on PM forces as those of bileaflet prolapse, these observations lead us to speculate that either our E-II valves represent a departure from clinical MVP, as E-II consisted of replacement with elongated neochordae of only 2 P2 neochordae, or that isolated PML prolapse may be more resistant to PM force increases due to repositioning of leaflet coaptation planes.

In aggregating our observations, we theorize that increased forces during prolapse is the result of increased leaflet surface area exposed to the ventricular pressure gradient. In particular, excessive leaflet surface area is a primary pathognomonic finding in Barlow's disease,²⁴ often observed with decreased coaptation lengths, as seen in patients with MVP. According to Pascal's Law, pressures are transmitted equally, undiminished, and in all directions within the left ventricle including the inferior MV, meaning that superior forces on the leaflets are correlated to the product of the ventricular pressure and the leaflet surface area exposed to that pressure. Because the chordae anchor the MV leaflets and transfer superiorly displaced forces from the leaflets to the PMs,^{21,25} we can assume that the aggregate increase in forces on the PMs is a result of the increased leaflet surface area from the billowing leaflets and reduced coaptation lengths, as the ventricular pressure remained constant throughout our experiments. When applied to the valvular system, this interaction leads to increased forces on the subvalvular apparatus and surrounding myocardium. This theory provides a plausible explanation for the statistically insignificant differences in forces for isolated PML prolapse valves, as our E-II model often shifted the coaptation plane anteriorly rather than increased the total leaflet surface area, which is additionally reflected in the insignificant differences in coaptation length between prolapsing and physiologic E-II valves.

Clinical Perspective

Our results establish new biomechanical understanding of MVP, potentially yielding larger implications in clinical translation for improved patient treatment, yet these extrapolated theories must first be clearly defined as speculative and hypothesis generating. Primarily, this work supports the development of a novel rationale towards MVP patient intervention with directed investigations aimed at better understanding the consequences of MVP in humans, with the goal of best defining which patients are candidates for intervention outside of current guidelines. Combined with findings in recent literature regarding sudden cardiac death in patients with prolapse in the absence of hemodynamic dysfunction, our data suggest that further investigations regarding earlier intervention of MVP patients, before severe MR serves as indication, may help develop a more informed approach toward addressing the downstream ventricular consequences of MVP by restoring healthy valve geometry and decreasing PM forces, particularly for patients with documented episodes of ventricular arrhythmia.^{6,8,11} Because we have shown that prolapse in the absence of significant MR can lead to potentially harmful forces on the PMs, we hypothesize that mere reduction of MR without restoring MV geometry and minimizing post-repair leaflet extension beyond the annulus height (i.e., billowing tissue) provides an insufficient method of MV repair. Such findings may have significant implications, for example, when comparing post-intervention leaflet morphology and subvalvular stress characteristics of post-surgical and transcatheter MV repairs.

Although our work was performed in the context of modeling MVP in the absence of hemodynamic dysfunction, our MVP models using our novel neochord length adjustment system, provide a novel research impetus into exploring the importance and consequences of achieving optimal neochord lengths during surgical repair. As shown, even millimeters of additional neochord lengthening can significantly alter the forces on the chordae and PMs, resulting in suboptimal repairs at risk of long-term fatigue damage and PM-level stretch-induced changes. Although work is required to further evaluate neochord length and PM forces, our novel adjustment system provides a platform to answer such questions in our ongoing investigations of MVP and its repair.

Limitations

Although we took many steps to minimize confounding factors and ensure optimal capture of native biomechanics, there were some key limitations to our work. The first limitation was the use of deceased large animal tissues as human MV models. While incorporation of porcine and ovine tissues in *ex vivo* experimentation has been well documented and validated in the literature, the use of such tissues introduced a level of temporal degradation, which could not be fully accounted for between experiments, as well as error in the differences in tissue composition and morphology between species and between healthy animal and pathological human valves. Although we ensured intra-experiment fidelity for our 3 models through randomized ordering, because the valve experiments were performed in a necessarily paired and progressive manner, we could not control for subsequent degradation of valve tissues between experiments. As such, we observed progressive decreases in overall PM force magnitudes between the different experimental models.

The second limitation was that our models did not fully capture the complexity of MVP, including annular dilation and excess leaflet tissue, and the use of artificial chordae may have impacted the magnitude of the results. Although MVP has a variety of etiologies, we chose to model PM displacement and chordal elongation, and although these are gross approximations of prolapsed states, we were able to recreate the main pathophysiologic phenotype of billowing leaflet tissue into the left atrium. However, more work is being done to integrate advances to ex vivo modeling of even chronic disease states such as annular dilation and changes to tissue properties,^{19,26} but for this focused study on prolapse biomechanics, exploring these additional etiologies were outside the scope of our research question.

Conclusions

In summary, we showed that bileaflet MVP results in significantly elevated forces and altered dynamics on the PMs, an increasingly pertinent and timely result that provides a plausible yet speculative mechanism for the stretch-induced changes in myocardial biology observed in certain patients with MVP. Moreover, this work calls for a new line of thinking regarding MVP, its treatment, and its consequences, which highlights the need for further investigations aimed at questioning the sufficiency of the sole reduction of MR without addressing the increased billowing leaflet surface area for an optimal repair, an important distinction especially amidst the rapid development of novel transcatheter devices. While further work aims to analyze PM forces in new models and under new conditions, this study establishes the basis for a more advanced biomechanical understanding of the changes involved in MVP.

Supplementary Material

Refer to Web version on PubMed Central for supplementary material.

Acknowledgements

The authors would like to thank the generous donation by Donald and Sally O'Neal to support this research effort.

Sources of Funding

Dr. Y Joseph Woo: NIH R01 HL152155

Dr. Yuanjia Zhu: Thoracic Surgery Foundation Resident Research Fellowship

Dr. Antonia van Kampen: American Heart Association Postdoctoral Fellowship

Dr. Robert A. Levine: American Heart Association Transformational Project Award

Dr. Yasufumi Nagata: American Society of Echocardiography Pamela Douglas Fellowship

Dr. Robert A. Levine: NIH R01-HL141917-04

Dr. Jordan E. Morningstar: NIH T32-HL007260-38

Abbreviations

MVP mitral valve prolapse

MV	mitral valve
MR	mitral regurgitation
PML	posterior mitral leaflet
PM(s)	papillary muscle(s)

References

1. Levine RA, Hagège AA, Judge DP, Padala M, Dal-Bianco JP, Aikawa E, Beaudoin J, Bischoff J, Bouatia-Naji N, Bruneval P, Butcher JT, Carpentier A, Chaput M, Chester AH, Clusel C, Delling FN, Dietz HC, Dina C, Durst R, Fernandez-Friera L, Handschumacher MD, Jensen MO, Jeunemaitre XP, Le Marec H, Le Tourneau T, Markwald RR, Mérot J, Messas E, Milan DP, Neri T, Norris RA, Peal D, Perrocheau M, Probst V, Pucéat M, Rosenthal N, Solis J, Schott J-J, Schwammenthal E, Slaugenhaupt SA, Song J-K, Yacoub MH, Leducq Mitral Transatlantic Network. Mitral valve disease--morphology and mechanisms. *Nat Rev Cardiol*. 2015;12:689–710. [PubMed: 26483167]
2. Waller BF, Morrow AG, Maron BJ, Del Negro AA, Kent KM, McGrath FJ, Wallace RB, McIntosh CL, Roberts WC. Etiology of clinically isolated, severe, chronic, pure mitral regurgitation: analysis of 97 patients over 30 years of age having mitral valve replacement. *Am Heart J*. 1982;104:276–288. [PubMed: 7102512]
3. Delling FN, Vasan RS. Epidemiology and pathophysiology of mitral valve prolapse: new insights into disease progression, genetics, and molecular basis. *Circulation*. 2014;129:2158–2170. [PubMed: 24867995]
4. Freed LA, Levy D, Levine RA, Larson MG, Evans JC, Fuller DL, Lehman B, Benjamin EJ. Prevalence and clinical outcome of mitral-valve prolapse. *N Engl J Med*. 1999;341:1–7. [PubMed: 10387935]
5. St John Sutton M, Weyman AE. Mitral valve prolapse prevalence and complications: an ongoing dialogue. *Circulation*. 2002;106:1305–1307. [PubMed: 12221042]
6. Basso C, Iliceto S, Thiene G, Perazzolo Marra M. Mitral valve prolapse, ventricular arrhythmias, and sudden death. *Circulation*. 2019;140:952–964. [PubMed: 31498700]
7. Sriram CS, Syed FF, Ferguson ME, Johnson JN, Enriquez-Sarano M, Cetta F, Cannon BC, Asirvatham SJ, Ackerman MJ. Malignant bileaflet mitral valve prolapse syndrome in patients with otherwise idiopathic out-of-hospital cardiac arrest. *J Am Coll Cardiol*. 2013;62:222–230. [PubMed: 23563135]
8. Basso C, Perazzolo Marra M, Rizzo S, De Lazzari M, Giorgi B, Cipriani A, Frigo AC, Rigato I, Migliore F, Pilichou K, Bertaglia E, Cacciavillani L, Bauce B, Corrado D, Thiene G, Iliceto S. Arrhythmic mitral valve prolapse and sudden cardiac death. *Circulation*. 2015;132:556–566. [PubMed: 26160859]
9. Morningstar JE, Gensemer C, Moore R, Fulmer D, Beck TC, Wang C, Moore K, Guo L, Sieg F, Nagata Y, Bertrand P, Spampinato RA, Glover J, Poelzing S, Gourdie RG, Watts K, Richardson WJ, Levine RA, Borger MA, Norris RA. Mitral valve prolapse induces regionalized myocardial fibrosis. *J Am Heart Assoc*. 2021;10:e022332. [PubMed: 34873924]
10. Sanfilippo AJ, Harrigan P, Popovic AD, Weyman AE, Levine RA. Papillary muscle traction in mitral valve prolapse: quantitation by two-dimensional echocardiography. *J Am Coll Cardiol*. 1992;19:564–571. [PubMed: 1538011]
11. Perazzolo Marra M, Basso C, De Lazzari M, Rizzo S, Cipriani A, Giorgi B, Lacognata C, Rigato I, Migliore F, Pilichou K, Cacciavillani L, Bertaglia E, Frigo AC, Bauce B, Corrado D, Thiene G, Iliceto S. Morphofunctional abnormalities of mitral annulus and arrhythmic mitral valve prolapse. *Circ Cardiovasc Imaging*. 2016;9:e005030. [PubMed: 27516479]
12. Fukuda S, Song J-K, Mahara K, Kuwaki H, Jang JY, Takeuchi M, Sun BJ, Kim YJ, Miyamoto T, Oginosawa Y, Sonoda S, Eto M, Nishimura Y, Takanashi S, Levine RA, Otsuji Y. Basal Left Ventricular Dilatation and Reduced Contraction in Patients With Mitral Valve Prolapse Can Be Secondary to Annular Dilatation: Preoperative and Postoperative Speckle-Tracking

Echocardiographic Study on Left Ventricle and Mitral Valve Annulus Interaction. *Circ Cardiovasc Imaging*. 2016;9:e005113. [PubMed: 27729364]

13. Hei S, Iwataki M, Jang J-Y, Kuwaki H, Mahara K, Fukuda S, Kim Y-J, Nabeshima Y, Onoue T, Nagata Y, Nishino S, Watanabe N, Takeuchi M, Nishimura Y, Song J-K, Levine RA, Otsuji Y. Possible mechanism of late systolic mitral valve prolapse: systolic superior shift of leaflets secondary to annular dilatation that causes papillary muscle traction. *Am J Physiol Heart Circ Physiol*. 2019;316:H629–H638. [PubMed: 30575434]
14. Park MH, Zhu Y, Imbrie-Moore AM, Wang H, Marin-Cuartas M, Paulsen MJ, Woo YJ. Heart valve biomechanics: the frontiers of modeling modalities and the expansive capabilities of ex vivo heart simulation. *Front Cardiovasc Med*. 2021;8:673689. [PubMed: 34307492]
15. Imbrie-Moore AM, Paulsen MJ, Thakore AD, Wang H, Hironaka CE, Lucian HJ, Farry JM, Edwards BB, Bae JH, Cutkosky MR, Woo YJ. Ex vivo biomechanical study of apical versus papillary neochoord anchoring for mitral regurgitation. *Ann Thorac Surg*. 2019;108:90–97. [PubMed: 30836099]
16. Imbrie-Moore AM, Park MH, Paulsen MJ, Sellke M, Kulkarni R, Wang H, Zhu Y, Farry JM, Bourdillon AT, Callinan C, Lucian HJ, Hironaka CE, Deschamps D, Joseph Woo Y. Biomimetic six-axis robots replicate human cardiac papillary muscle motion: pioneering the next generation of biomechanical heart simulator technology. *J R Soc Interface*. 2020;17:20200614. [PubMed: 33259750]
17. Ostli B, Vester-Petersen J, Askov JB, Hønge JL, Levine RA, Høge A, Nielsen SL, Hasenkam JM, Nygaard H, Jensen MO. In vitro system for measuring chordal force changes following mitral valve patch repair. *Cardiovasc Eng Technol*. 2012;3:263–268. [PubMed: 26273417]
18. Jensen MO, Fontaine AA, Yoganathan AP. Improved in vitro quantification of the force exerted by the papillary muscle on the left ventricular wall: three-dimensional force vector measurement system. *Ann Biomed Eng*. 2001;29:406–413. [PubMed: 11400721]
19. Imbrie-Moore AM, Paulsen MJ, Zhu Y, Wang H, Lucian HJ, Farry JM, MacArthur JW, Ma M, Woo YJ. A novel cross-species model of Barlow's disease to biomechanically analyze repair techniques in an ex vivo left heart simulator. *J Thorac Cardiovasc Surg*. 2021;161:1776–1783. [PubMed: 32249088]
20. Jimenez JH, Soerensen DD, He Z, Ritchie J, Yoganathan AP. Effects of papillary muscle position on chordal force distribution: an in-vitro study. *J Heart Valve Dis*. 2005;14:295–302. [PubMed: 15974521]
21. Paulsen MJ, Bae JH, Imbrie-Moore AM, Wang H, Hironaka CE, Farry JM, Lucian H, Thakore AD, Cutkosky MR, Joseph Woo Y. Development and Ex Vivo Validation of Novel Force-Sensing Neochoordae for Measuring Chordae Tendineae Tension in the Mitral Valve Apparatus Using Optical Fibers With Embedded Bragg Gratings. *J Biomech Eng*. 2020;142:0145011–9. [PubMed: 31253992]
22. Constant Dit Beaufile A-L, Huttin O, Jobbe-Duval A, Senage T, Filippetti L, Piriou N, Cuffe C, Venner C, Mandry D, Sellal J-M, Le Scouarnec S, Capoulade R, Marrec M, Thollet A, Beaumont M, Hossu G, Toquet C, Gourraud J-B, Trochu J-N, Warin-Fresse K, Marie P-Y, Schott J-J, Roussel J-C, Serfaty J-M, Selton-Suty C, Le Tourneau T. Replacement myocardial fibrosis in patients with mitral valve prolapse: relation to mitral regurgitation, ventricular remodeling, and arrhythmia. *Circulation*. 2021;143:1763–1774. [PubMed: 33706538]
23. Gunning GM, Murphy BP. Characterisation of the fatigue life, dynamic creep and modes of damage accumulation within mitral valve chordae tendineae. *Acta Biomater*. 2015;24:193–200. [PubMed: 26087111]
24. Melnitchouk SI, Seeburger J, Kaeding AF, Misfeld M, Mohr FW, Borger MA. Barlow's mitral valve disease: results of conventional and minimally invasive repair approaches. *Ann Cardiothorac Surg*. 2013;2:768–773. [PubMed: 24349980]
25. Askov JB, Hønge JL, Jensen MO, Nygaard H, Hasenkam JM, Nielsen SL. Significance of force transfer in mitral valve-left ventricular interaction: in vivo assessment. *J Thorac Cardiovasc Surg*. 2013;145:1635–41, 1641.e1. [PubMed: 22980066]
26. Imbrie-Moore AM, Zhu Y, Bandy-Vizcaino T, Park MH, Wilkerson RJ, Woo YJ. Ex vivo model of ischemic mitral regurgitation and analysis of adjunctive papillary muscle repair. *Ann Biomed Eng*. 2021;49:3412–3424. [PubMed: 34734363]

What is Known

- Recent studies have linked mitral valve prolapse to localized myocardial fibrosis, ventricular arrhythmia, and even sudden cardiac death independent of mitral regurgitation or hemodynamic dysfunction.
- The primary mechanistic theory is rooted in increased papillary muscle traction and forces due to prolapse; yet no biomechanical evidence exists showing increased forces.

What the Study Adds

- We discovered that bileaflet prolapse, absent of hemodynamic dysfunction, results in significantly elevated forces and altered dynamics on the papillary muscles, an increasingly pertinent and timely result that provides a plausible mechanism for the stretch-induced changes in myocardial biology observed in certain patients with mitral valve prolapse.
- Our work has deep clinical implications in the treatment of mitral valve prolapse, suggesting that the sole reduction of mitral regurgitation without addressing the increased billowing leaflet surface area is insufficient for an optimal repair, an important distinction especially amidst the rapid development of novel transcatheter devices.
- While further work aims to analyze papillary muscle forces in new models and under new conditions, this study establishes the basis for a more advanced biomechanical understanding of the changes involved in mitral valve prolapse.

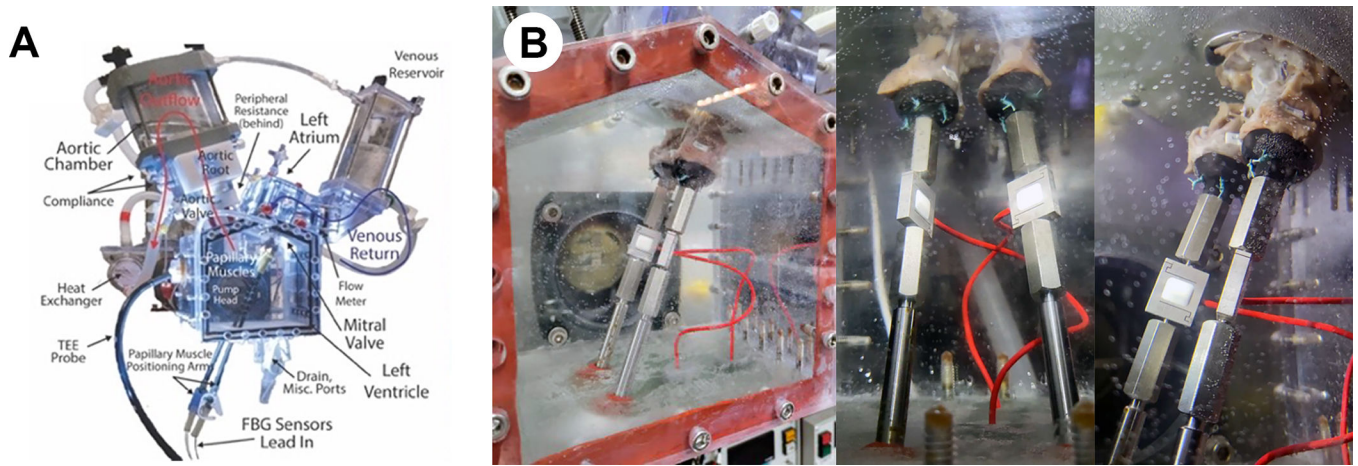


Figure 1.

(A) Labeled diagram of the *ex vivo* left heart simulator. (B) Images of our custom papillary muscle force transduction system integrated within the left heart simulator. Submersible force transducers were mounted to stainless steel rods transecting the gasketed bottom of the ventricular chamber, allowing for water-tight, exterior adjustability of the papillary muscle positioning. The force sensors set at a sampling rate of 1.2 kHz can record forces with an ultimate resolution on the order of hundreds of μN .

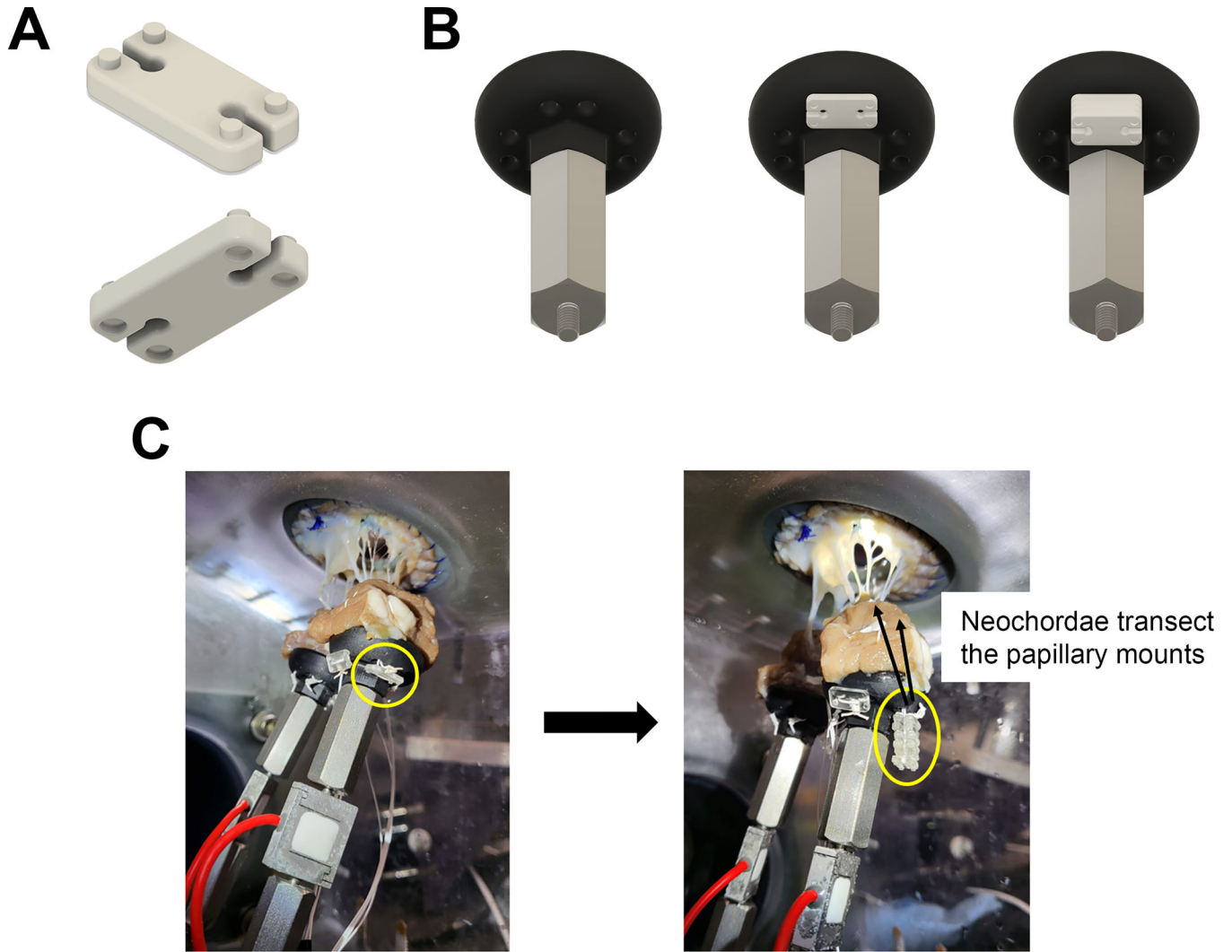


Figure 2.

Computer-aided designs of our novel neochord length adjustment system. (A) Designs of our stackable, interlocking, plastic pledgets that were three-dimensionally printed using a high resolution, digital light synthesis printer. Each pledget had a precise thickness of 1.5 mm and contained four embossed and debossed cylinder features, allowing for vertical stacking. (B) Neochord length adjustment system integrated with custom PM mounts. GoreTex neochord sutures were routed through the mounts and pledgets such that pledgets could easily be stacked or removed on the bottom of the mounts to either shorten or lengthen the neochordae. (C) Images demonstrating stacking pledgets. The transected pledgets and mounts allow for adjustments in neochordae lengths. We used this system to precisely generate and tune our leaflet-specific prolapse models.

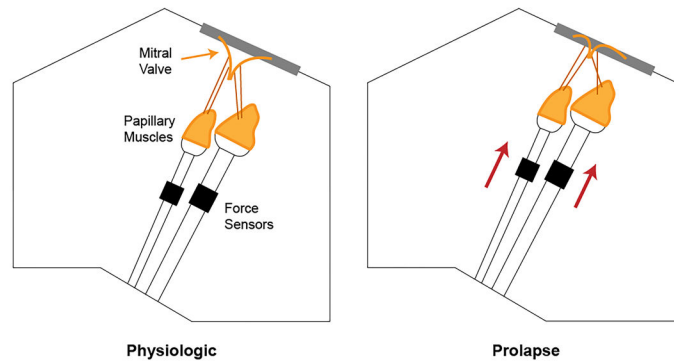
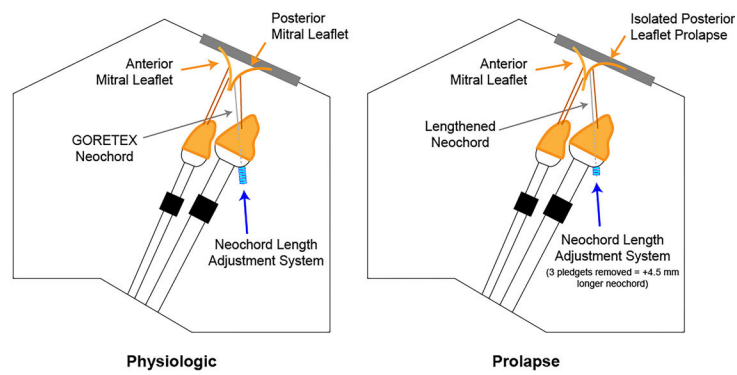
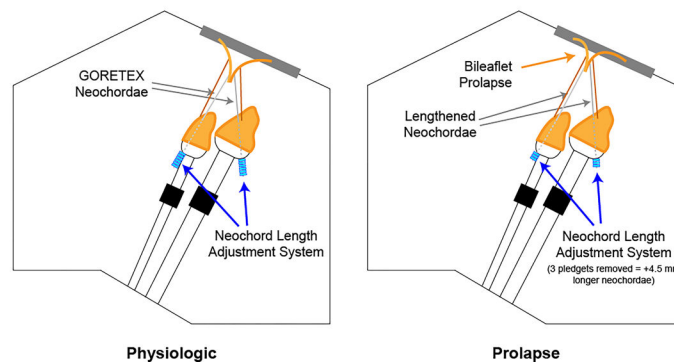
A. Experiment 1 (E-I): Bileaflet Prolapse from Papillary Muscle Displacement**B. Experiment 2 (E-II): Isolated Posterior Mitral Leaflet Prolapse from Neochord Length Adjustment****C. Experiment 3 (E-III): Bileaflet Prolapse from Neochord Length Adjustment**

Figure 3. Labeled schematic illustrations of experimental procedures. **(A)** Schematic of Experiment-I where bileaflet prolapse was induced using a model of superior papillary muscle displacement. **(B)** Schematic of Experiment-II where isolated posterior mitral leaflet prolapse was induced using our novel neochord length adjustment system. P2 primary chordae were excised and replaced with two posterior mitral leaflet neochordae to each papillary muscle and lengthened or shortened for prolapse or physiologic conditions. **(C)** Schematic of Experiment-III where bileaflet prolapse was induced using our neochord

length adjustment system. A2 primary chordae were excised from the same valve in Experiment-II and two neochordae were implanted to the anterior mitral leaflet and each papillary muscle and lengthened or shortened for prolapse or physiologic conditions.

Author Manuscript

Author Manuscript

Author Manuscript

Author Manuscript

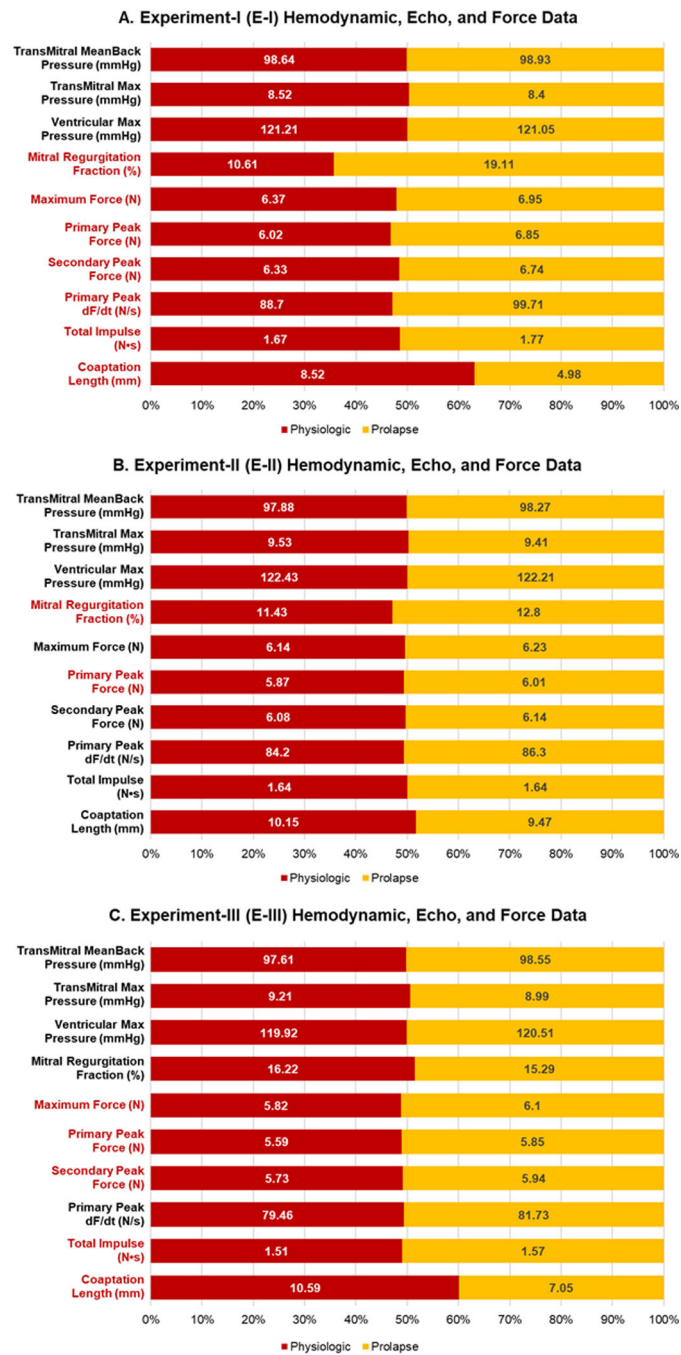


Figure 4. Hemodynamic, force, and echocardiographic data presented as stacked binomial bar plots for (A) Experiment-I, (B) Experiment-II, and (C) Experiment-III. Categories with significant differences ($p < 0.05$) are highlighted in red.

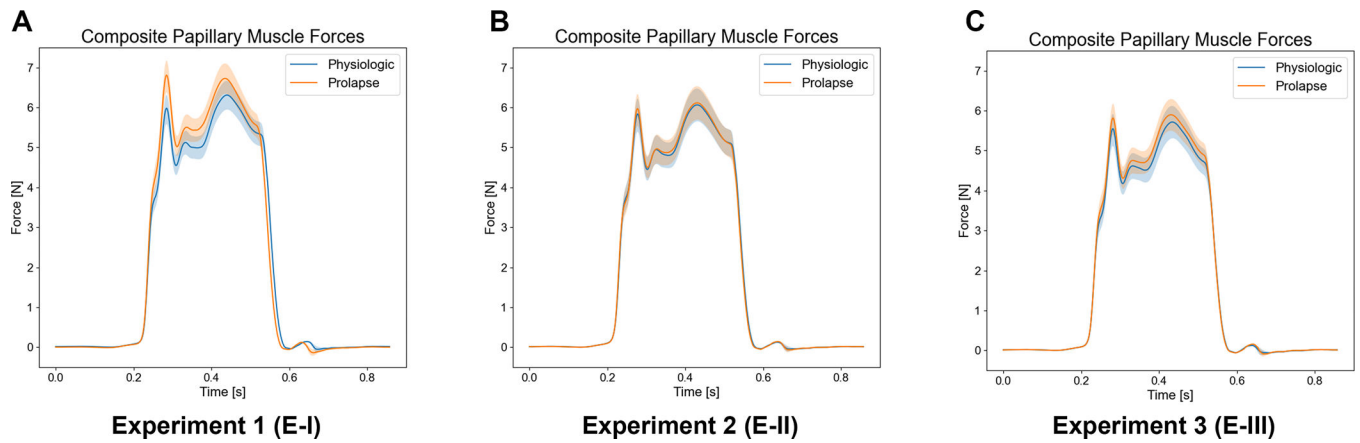


Figure 5. Composite papillary muscle force profiles for the intra-cardiac time domain. **(A)** Experiment-I composite papillary muscle force profiles for a single cardiac cycle averaged across all samples for each condition. Note the difference in force profiles due to the higher primary peak magnitudes for prolapsing valves. **(B)** Experiment-II composite papillary muscle force profiles for a single cardiac cycle averaged across all samples for each condition. **(C)** Experiment-III composite papillary muscle force profiles for a single cardiac cycle averaged across all samples for each condition.

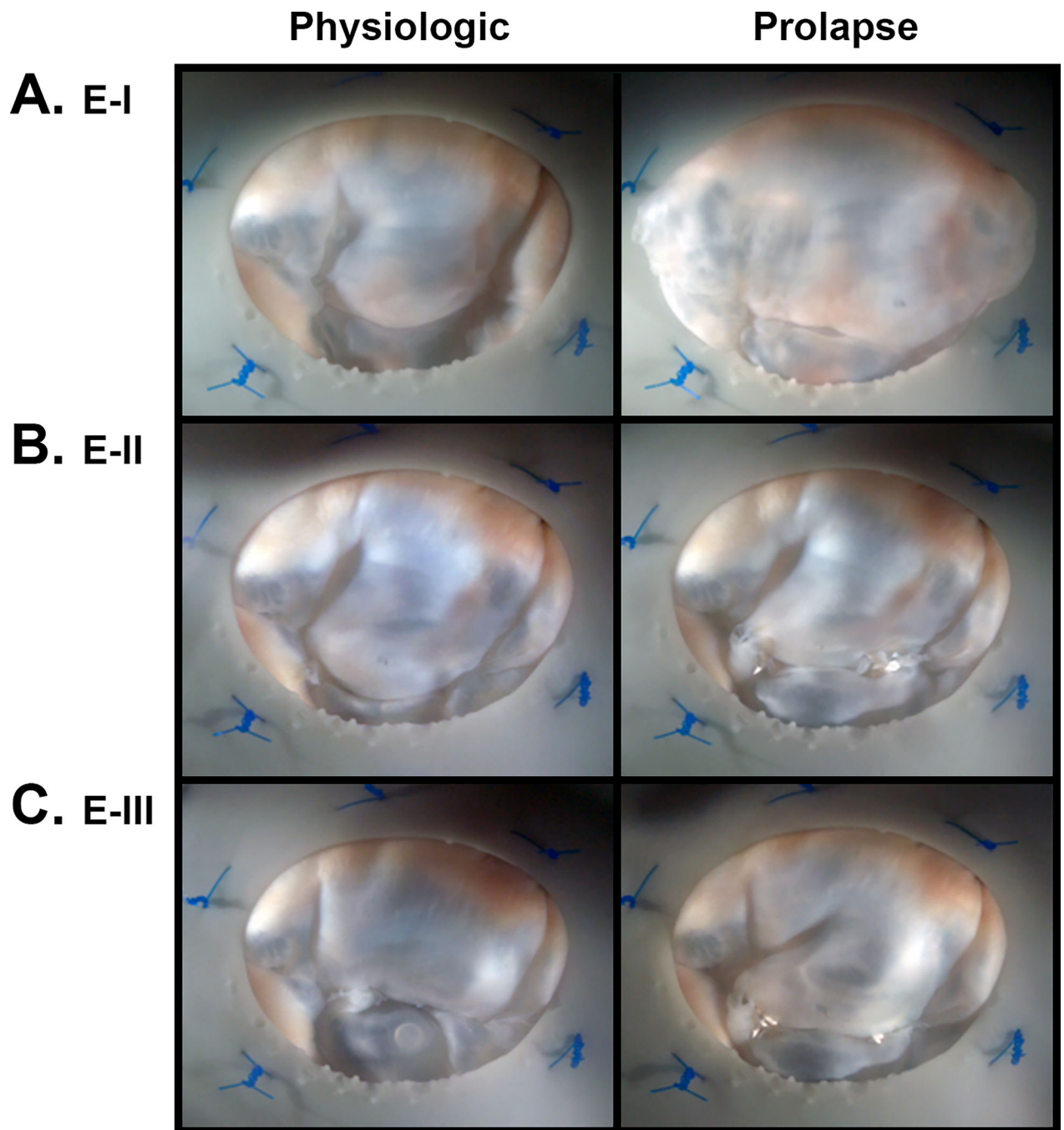


Figure 6. Representative paired images taken from the surgeon's view of the mitral valve for both physiologic and prolapse conditions in experiments (A) Experiment-I (E-I), (B) Experiment-II (E-II), and (C) Experiment-III (E-III). Note, in particular, that increased neochord lengths for prolapsing Experiment-II valves results in an anteriorly-shifted coaptation plane rather than excess billowing leaflet tissue.

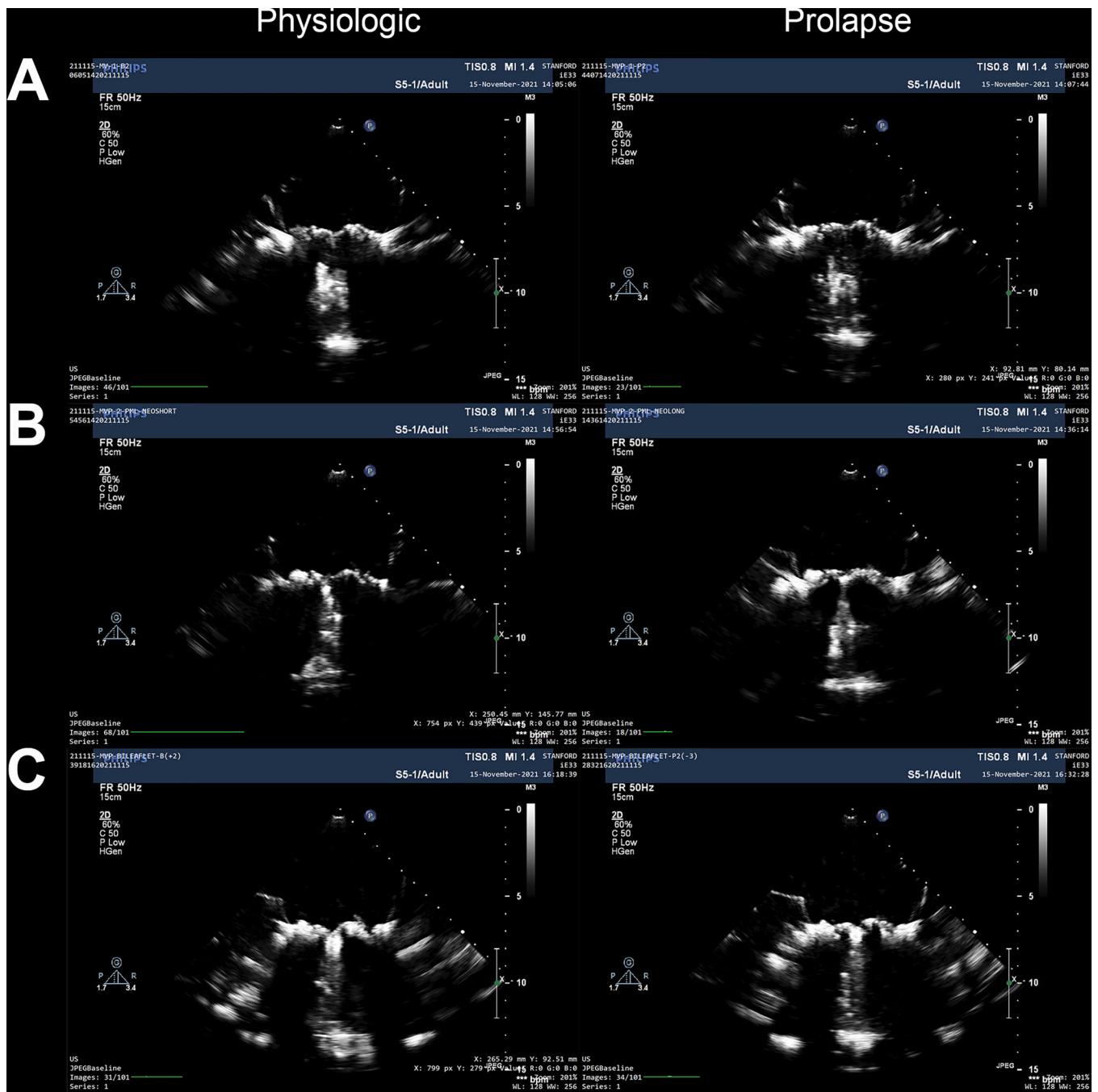


Figure 7. Representative two dimensional echocardiography image stills of the mitral valve during systole. Images include long-axis views for both physiologic and prolapse conditions for (A) Experiment-I, (B) Experiment-II, and (C) Experiment-III.